PROCEEDINGS OF SPIE

SPIEDigitalLibrary.org/conference-proceedings-of-spie

Thermal characterisation of quantum cascade lasers with Fabry Perot modes

Sinan Gündoğdu, Hadi Sedaghat Pisheh, Abdullah Demir, Mete Günoven, Atilla Aydinli, et al.

Sinan Gündoğdu, Hadi Sedaghat Pisheh, Abdullah Demir, Mete Günoven, Atilla Aydinli, Carlo Sirtori, "Thermal characterisation of quantum cascade lasers with Fabry Perot modes," Proc. SPIE 10682, Semiconductor Lasers and Laser Dynamics VIII, 106820J (9 May 2018); doi: 10.1117/12.2311651

SPIE.

Event: SPIE Photonics Europe, 2018, Strasbourg, France

Thermal characterisation of quantum cascade lasers with Fabry Perot modes

Sinan Gündoğdu[a], Hadi Sedaghat Pisheh[b], Abdullah Demir[c], Mete Günoven[d], Atilla Aydınlı[*e], and Carlo Sirtori[f]

[a]Physics Department, Bilkent University, Ankara 06800, Turkey
[b]Mechanical Engineering Department, Bilkent University, Ankara 06800, Turkey
[c]National Nanotechnology Research Center, Bilkent University, Ankara 06800, Turkey
[d]Physics Department, Middle East Technical University, Ankara 06800, Turkey
[e]Electrical and Electronics Engineering Department, Uludag University, Bursa, 16059 Turkey
[f]Laboratoire Matériaux et Phénomènes Quantiques, Université Paris Diderot-Paris7, Paris, France

ABSTRACT

Quantum cascade lasers are coherent light sources that rely on intrersubband transition in periodic semiconductor quantum well structures. They operate at frequencies from mid-infrared to terahertz. In cases of long wavelength and typical low thermal conductivity of the active region, temperature rise in the active region during operation is a major concern. Thermal conductivity of QCL epi-layers differ significantly from the values of bulk semiconductors and measurement of the thermal conductivity of epi-layers is critical for design. It is well known that Fabry-Perot spectra of QCL cavities exhibit fine amplitude oscillations with frequency and can be used for real time in-situ temperature measurement. Phase of the modulation depends on the group refractive index of the cavity, which depends on the cavity temperature. We fabricated QCL devices with from 12, to 24 um mesa widths and 2mm cavity length and and measured high resolution, high speed time resolved spectra using a FTIR spectrometer in step scan mode in a liquid nitrogen cooled, temperature controlled dewar. We used the time resolved spectra of QCLs to measure average temperature of the active region of the laser as a function of time. We examined the effect of pulse width and duty cycle on laser heating. We measured the temperature derivative of group refractive index of the cavity. Building a numerical model, we estimated the thermal conductivity of active region and calculated the heating of the QCL active region in pulsed mode for various waveguide widths.

Keywords: Quantum Cascade Lasers, Thermal Conductivity, Temperature

1. INTRODUCTION

Quantum cascade lasers (QCLs) are semiconductor devices that can be tailored to emit light from infrared to terahertz frequencies. They rely on intersubband transitions of multi-quantum wells formed by many layers of semiconductors, hence they can lase at photon energies less than the band-gap of the materials. Since their first demonstration in 1994,[1] extensive efforts has been made to increase efficiency, high temperature operation and high power output.[2] Since their relatively thick active region formed by many layers of alternating semiconductors, their thermal behavior is different than other semiconductor lasers like diode lasers. Thermal conductivity of active region is less than the bulk materials constituting it and strongly anisotropic.[3] Since the energy difference between the intersubband levels is low, they can be easily excited with thermal energy of the lattice. Therefore their operation depends on temperature strongly. For this reason, thermal management of QCLs is an important factor for the design of a QCL and its packaging.[4]

In-situ temperature measurement of a QCL active region yields valuable information about the thermal performance and heat dissipation of the laser. Some methods that has been used to measure temperature of QCLs include microprobe photoluminescence (PL),[3,5–7] and thermoreflectance.[8–11] Photoluminescence peak wavelength of the semiconductors depends on temperature. For PL method, slight wavelength shift of the peak is measured by focusing an excitation laser on the facet and collecting the emitted PL light and analyzing the light with a spectrometer. By scanning the focused laser over the facet, a 2D map of temperature can be obtained.

Semiconductor Lasers and Laser Dynamics VIII, edited by Krassimir Panajotov, Marc Sciamanna, Rainer Michalzik,
Proc. of SPIE Vol. 10682, 106820J · © 2018 SPIE · CCC code: 0277-786X/18/$18 · doi: 10.1117/12.2311651

However, PL light signal can be weak and measurement may require long integration times. Thermoreflectance measurements use a measurement setup similar to microprobe PL, but measure the change in reflectivity due to temperature by measuring the reflected light intensity from the surface. Reflectivity variation with temperature is in the order of $10^{-3}K^{-1}$, therefore this method also requires long integration times.

The method we present in this study uses fast, time resolved FTIR spectra of a QCLs to measure the temperature within the laser cavity. A typical Fabry-Perot (FP) cavity laser has spectral modulation in its spectrum with a period of;

$$\Delta f = \frac{1}{2dn_g} \ , \tag{1}$$

where Δf is the difference between two successive peak frequencies, d is the cavity length, and n_g is the group refractive index. Peak frequencies are;

$$f = \frac{m}{2dn_g} \ , \tag{2}$$

where m is an integer and typically in the order of 10^3 for QCLs. Since the refractive index of the laser cavity depends on temperature, peak frequencies shift as the laser heats. QCL emission is has a high spectral brightness compared to PL, so time resolved temperature measurement can be done in a time efficient way. Another advantage of this method is that it only requires a FTIR with a fast MCT detector which is used for measurement of QCL spectra prevalently.

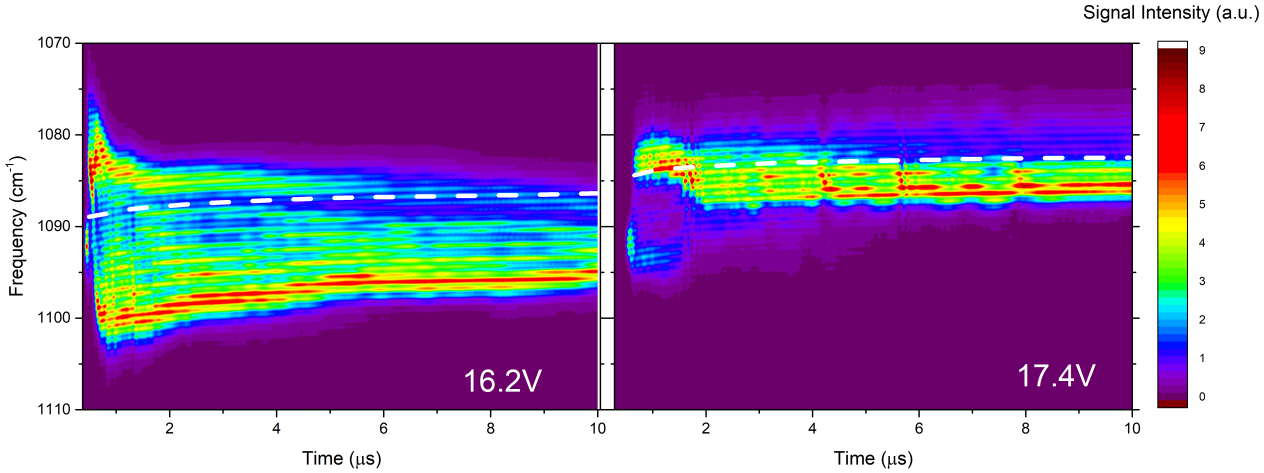

Figure 1. Time resolved spectra of a QCL measured at 16.2V and 17.4V voltage pulses initiated at time=0. White dashed line indicates the shift of the FP modes with time.

2. EXPERIMENTAL

For QCL crystals, we used a design similar to 3-phonon resonant InGaAs-AlInAs based structure developed by Wang et. al.[12] Epitaxial structure of the crystal is; 100nm InGaAs(5E18) / 850nm InP(5E18) / 2500nm InP (5E16) / 200nm InGaAs (5E18) / Active region / 200nm InGaAs(5E18) / 2000nm InP(5E16) / 50nm InGaAs(1E18)/ Buffer InP (5E18)/Substrate InP(5E18). We wet etched the crystals to form 12, 16, 20 and 24 μm wide waveguides (width at the top of the mesa). We used 400 nm PECVD silicon nitride to insulate the wafer and evaporated Ti/Au 20/100nm as the top contact and GeAu/Ni/Au 40/40/150nm as the bottom contact. Top contact was also electroplated with $5\mu m$ gold for better heat dispersion. The laser bars were cleaved into 2mm long cavities. The lasers were mounted on a liquid nitrogen cooled, temperature controlled dewar and voltage pulses were applied with a voltage pulser at 0.1% duty cycle.

Spectrum of the QCLs were measured using a Bruker Vertex 70v FTIR spectrometer with a fast MCT photodetector. The laser light was collimated with a gold parabolic mirror and coupled into side input port of

the spectrometer. The spectrometer was operated in step-scan mode, which means that the interferometer stops at each interferogram position and records a time resolved optical signal. The spectrometer begins recording the signal when initiated by the trigger output of the voltage pulser. Spectrometer was set to record 100 repetitions and calculate the average of these before moving to the next interferogram position.

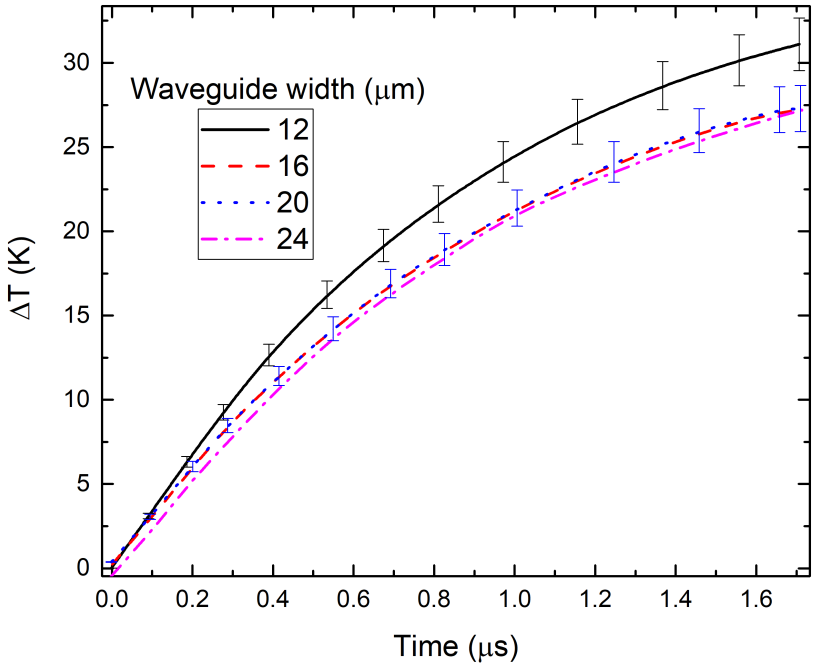

Figure 2. Mesa width vs measured temperature rise as a function of time.

3. RESULTS AND DISCUSSION

Figure 1 shows example spectra of a 12um wide QCL lasing with $10\mu s$ voltage pulses with amplitude of 16.2V and 17.4V. Heatsink temperature is -160°C. Time scale begins at the beginning of the voltage pulse. The gain spectrum of the QCL crystal depends on both temperature and voltage. For this reason, the two spectra are very different than each other. However, both share the same features of periodic modulation with period of $\approx 0.78\text{cm}^{-1}$, which are due to longitudinal FP modes. These modes shift over time due to heating of the cavity. This is indicated in the figure with white dashed lines.

To extract the frequency shift of the modes accurately, we used the following procedure; We first calculated the Fourier transform amplitudes of the spectrum and found the peak that corresponds to the period of the FP modes, which is approximately 1.28cm for these lasers. Then we calculated the phase of the Fourier transform of the spectrum at 1.28cm, for all time slices. Finally, we "unwrapped" the phase as a function of time, by means of adding or subtracting 2π to the phases to fix the discontinuities in phase with respect to time.

To calibrate the frequency shift of the FP modes with temperature, we measured the spectrum of the lasers at varied heatsink temperatures from -160°C to -120°C and measured the phases. We have found that the frequency shift is 3.6×10^{-2} $\text{cm}^{-1}/°\text{C}$ for these 2mm long lasers. Using this calibration constant, we calculated the temperatures as a function of time using the FP shifts for various lasers.

Fig. 2 shows the measured temperature rise as a function of time, starting from the initiation of the lasing, for lasers with different cavity widths. An estimated error of 5% due to current density variation is shown. These

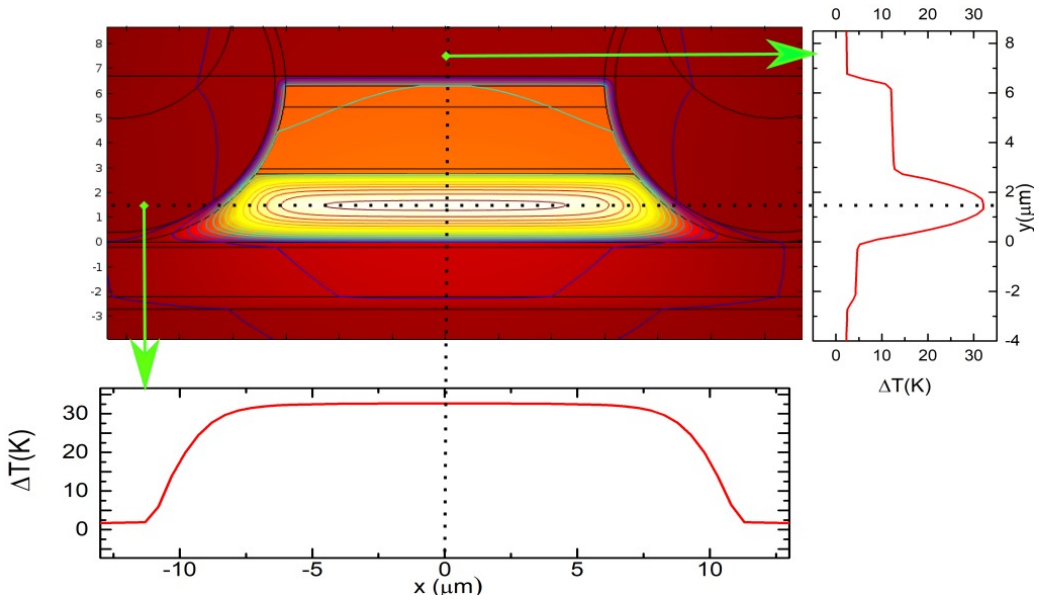

Figure 3. Calculated 2D temperature rise map of a 16μm laser and temperature rise at two cross-sections indicated in the figure with dashed lines.

measurements were done with 17V 2μs pulses. At t=0, laser temperature is equal to heatsink temperature -160°, and increases up to 30C° at 1.7μs with a gradually decreasing rate. temperature of 16,20 and 24 μm lasers are very close to each other, and the 12μm laser heats up about 10% more. Which may be due to current densities of the lasers not being exactly equal, probably due to series resistances, or non-uniform current flow due to wet etched waveguide profiles. Another reason may be the optical modes of the cavity. For narrower waveguides, cavity supports a single fundamental mode, with maximum mode intensity at the center of the cavity. As the cavity becomes wider, higher order modes appear and these modes have different distribution than the fundamental mode. The 12μm laser may appear warmer since it is closer to single mode operation, and the light we measure passes mostly through the center of the cavity, which is hotter than the edges.

To examine the relationship between the cavity width and the temperature rise, we built a 2D time dependent model of the laser using Comsol Multiphysics. We defined temperature dependent thermal conductivities and specific heats of the bulk materials such as cladding, insulator silicon nitride, and gold. Thermal properties of these materials listed elsewhere.[13] A heat source is defined on the active region with constant power density. Thermal conductivity of the active region was defined as a fitting parameter and it was varied to minimize the difference between temperatures calculated by the model and the experimentally measured values. The details of the fitting process may also be found in the previous work.[13] A best fit was obtained for 2.1±1W/m.K. Fig. 3 shows the calculated temperature distribution of 16μm wide laser at 55kW/mm^3 heat source at the active region at t=1.8μs after the pulse begins. Temperature profiled at cross-sections from the center of the active region is also shown. Temperature rise is mostly confined in the active region, since it has much lower thermal conductivity than the InP and Gold. Temperature distribution at the center of the cavity along the x-axis is almost constant and immediately drops near the gold layer. However, in the y-axis temperature sharply increases at the active region. Since the temperature gradient at the x-axis is lower, most of the heat in the center of the active region flows in the substrate direction. At y=-2μm a step in Temperature is due to thermal barrier of low thermal conductivity InGaAs layer. We calculated the average temperatures of the active region for various waveguide widths. The results has been depicted in a seperate figure for clarity; Fig. 4 shows the Temperature rise as a function of time for various laser widths. For 20-28μm, average temperature rises are almost identical, as we observed in Fig. 2. Temperature rise for 12μm laser is somewhat lower, since the ratio of heat flowing to the sides, where the electroplated gold spreads the heat.

It is also possible to measure the temperature dependence of the group refractive index of a QCL cavity with

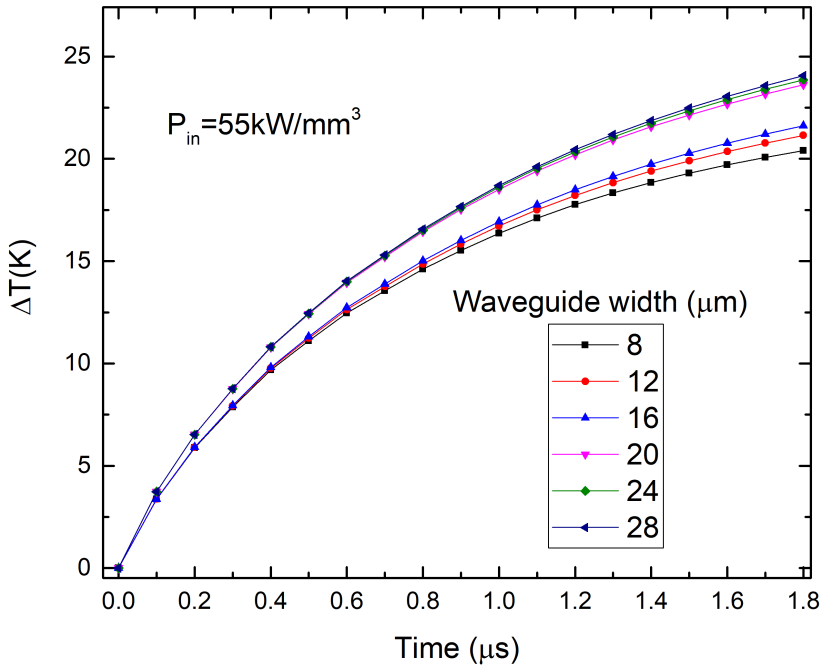

Figure 4. Calculated temperatures as a function of time for different mesa widths.

this method. Since $\Delta f = 1/1.28cm = 0.78cm^{-1}$, from equation 1, $n_g = 3.21$, from equation 2, $m \approx 1400$. By taking the temperature derivative of 2, we calculate;

$$\frac{dn_g}{dT} = -\frac{2dn_g^2}{m}\frac{df}{dT} \approx 3.3 \times 10^{-5} K^{-1} \tag{3}$$

Which is a reasonable value since for bulk InP and GaAs, $dn/dT \approx 7 \times 10^{-5}$.[14]

Time resolved spectrum of a QCL yields valuable information for physics of QCLs. We have demonstrated the measurement of temperature of QCLs with various width. We have shown that for larger than 16 μm wide waveguides, difference in temperature rise in pulsed operation is not strongly dependent on waveguide width. We have calculated the thermal conductivity of InGaAs/AlInAs based QCL active region structure as 2.1 W/m.K, group refractive index of a 12 μm wide cavity as 3.21, and temperature derivative of the group refractive index as $3.3 \times 10^{-5} K^{-1}$. Analysis of longitudinal Fabry Perot modes in QCL spectrum is a convenient method for measurement of these properties.

ACKNOWLEDGMENTS

We thank Turkish Scientific and Technological Research Agency (TUBITAK) for financial support under grant no: SANTEZ, 0573.STZ.2013-2

REFERENCES

[1] Faist, J., Capasso, F., Sivco, D. L., Sirtori, C., Hutchinson, A. L., and Cho, A. Y., "Quantum cascade laser," *Science* **264**, 553–556 (apr 1994).

[2] Vitiello, M. S., Scalari, G., Williams, B., and Natale, P. D., "Quantum cascade lasers: 20 years of challenges," *Optics Express* **23**, 5167 (feb 2015).

[3] Vitiello, M. S. and Scamarcio, G., "Anisotropic heat propagation velocity in quantum cascade lasers," *Applied Physics Letters* **96**, 101101 (mar 2010).

[4] Spagnolo, V., Lops, A., Scamarcio, G., Vitiello, M. S., and Franco, C. D., "Improved thermal management of mid-IR quantum cascade lasers," *Journal of Applied Physics* **103**, 043103 (feb 2008).

[5] Spagnolo, V., Scamarcio, G., Marano, D., Troccoli, M., Capasso, F., Gmachl, C., Sergent, A., Hutchinson, A., Sivco, D., Cho, A., Page, H., Becker, C., and Sirtori, C., "Thermal characteristics of quantum-cascade lasers by micro-probe optical spectroscopy," *IEE Proceedings - Optoelectronics* **150**(4), 298 (2003).

[6] Fathololoumi, S., Ban, D., Luo, H., Dupont, E., Laframboise, S. R., Boucherif, A., and Liu, H. C., "Thermal behavior investigation of terahertz quantum-cascade lasers," *IEEE Journal of Quantum Electronics* **44**, 1139–1144 (dec 2008).

[7] Vitiello, M. S., Scamarcio, G., and Spagnolo, V., "Temperature dependence of thermal conductivity and boundary resistance in THz quantum cascade lasers," *IEEE Journal of Selected Topics in Quantum Electronics* **14**(2), 431–435 (2008).

[8] Pierściński, K., Pierścińska, D., Iwińska, M., Kosiel, K., Szerling, A., Karbownik, P., and Bugajski, M., "Investigation of thermal properties of mid-infrared AlGaAs/GaAs quantum cascade lasers," *Journal of Applied Physics* **112**, 043112 (aug 2012).

[9] Pierścińska, D., Pierściński, K., Płuska, M., Marona, Ł., Wiśniewski, P., Perlin, P., and Bugajski, M., "Examination of thermal properties and degradation of InGaN - based diode lasers by thermoreflectance spectroscopy and focused ion beam etching," *AIP Advances* **7**, 075107 (jul 2017).

[10] Pierścińska, D., Kozlowska, A., Pierściński, K., Bugajski, M., Tomm, J. W., Ziegler, M., and Weik, F., "Thermal processes in high-power laser bars investigated by spatially resolved thermoreflectance," *Journal of Materials Science: Materials in Electronics* **19**, 150–154 (mar 2008).

[11] Pierścińska, D., Pierściński, K., Morawiec, M., Karbownik, P., Gutowski, P., and Bugajski, M., "CCD thermoreflectance spectroscopy as a tool for thermal characterization of quantum cascade lasers," *Semiconductor Science and Technology* **31**, 115006 (sep 2016).

[12] Wang, Q. J., Pflügl, C., Diehl, L., Capasso, F., Edamura, T., Furuta, S., Yamanishi, M., and Kan, H., "High performance quantum cascade lasers based on three-phonon-resonance design," *Applied Physics Letters* **94**, 011103 (jan 2009).

[13] Gundogdu, S., Pisheh, H. S., Demir, A., Gunoven, M., Aydinli, A., and Sirtori, C., "Time resolved fabry-perot measurements of cavity temperature in pulsed QCLs," *Optics Express* **26**, 6572 (mar 2018).

[14] Cherroret, N., Chakravarty, A., and Kar, A., "Temperature-dependent refractive index of semiconductors," *Journal of Materials Science* **43**, 1795–1801 (Mar 2008).